SLAC-PUB-12785
September 2007

CGRaBS: An All-Sky Survey of Gamma-Ray Blazar Candidates

Stephen E. Healey[1], Roger W. Romani[1], Garret Cotter[2], Peter F. Michelson[1], Edward F. Schlafly[1], Anthony C. S. Readhead[3], Paolo Giommi[4], Sylvain Chaty[5], Isabelle A. Grenier[5], Lawrence C. Weintraub[3]

ABSTRACT

We describe a uniform all-sky survey of bright blazars, selected primarily by their flat radio spectra, that is designed to provide a large catalog of likely γ-ray AGN. The defined sample has 1625 targets with radio and X-ray properties similar to those of the EGRET blazars, spread uniformly across the $|b| > 10^\circ$ sky. We also report progress toward optical characterization of the sample; of objects with known $R < 23$, 85% have been classified and 81% have measured redshifts. One goal of this program is to focus attention on the most interesting (e.g., high redshift, high luminosity, ...) sources for intensive multiwavelength study during the observations by the Large Area Telescope (LAT) on *GLAST*.

Subject headings: BL Lacertae objects: general — galaxies: active — quasars: general — surveys

1. Introduction

It is well-known (Hartman et al. 1999; Mattox et al. 2001) that many of the high-latitude EGRET sources are associated with the bright, flat radio spectrum AGN known as blazars. Sowards-Emmerd et al. (2003; SRM03) quantified such associations, developing a combined figure of merit (FoM), which measured the likelihood that an individual radio/X-ray source near the large ($\sim$0.7°) Third EGRET Catalog (3EG, Hartman et al. 1999) uncertainty regions

[1]Department of Physics/KIPAC, Stanford University, Stanford, CA 94305; sehealey@astro.stanford.edu, rwr@astro.stanford.edu.

[2]Department of Astrophysics, University of Oxford, Oxford OX1 3RH, UK

[3]Department of Astronomy, California Institute of Technology, Pasadena, CA 91125

[4]ASI Science Data Center, I-00044 Frascati, Italy

[5]Laboratoire AIM, CEA/DSM - CNRS - Université Paris Diderot, Service d'Astrophysique, CEA Saclay, 91191 Gif/Yvette, France

Submitted to The Astrophysical Journal Supplement Series

Work supported in part by US Department of Energy contract DE-AC02-76SF00515

is the γ-ray counterpart. They also noted that there are many radio-loud blazars with very similar properties not obviously associated with a 3EG source. A likely explanation is that blazars are very variable at high energy, with duty cycles for the bright, flaring state as small as a few percent (Hartman et al. 1993; Kniffen et al. 1993). During the limited (typically two weeks per pointing direction) 3EG exposure many of these sources may have been in quiescence. Accordingly, Sowards-Emmerd et al. (2005) extended the SRM03 analysis by selecting "3EG-like" blazars, i.e., sources whose radio flux density and spectrum (and X-ray flux) were very like those of the 3EG blazars but which happened not to lie within a 3EG test statistic (TS) uncertainty region. The positions of these sources showed a clear excess of γ-ray photons over background and these sources are likely to show γ-ray high states during future missions.

The Large Area Telescope (LAT) on *GLAST* will provide an improvement of several orders of magnitude over EGRET/*CGRO* with an increased sensitivity in the 50 MeV − 300 GeV range and a wide (>2.5 sr) field of view. The LAT should detect many thousands of sources during the 5- to 10-year mission, with a large fraction of the high-latitude sources being blazars. The early mission will be devoted to a sky survey, covering the entire sky at good sensitivity every three hours. This will greatly enhance the likelihood of detecting transient and variable sources, such as blazars. While several large samples of blazars have been compiled recently (see especially the ASDC blazar catalog, Massaro et al. 2007, and the ROXA catalog, Turriziani et al. 2007), there is a surprisingly incomplete knowledge of the radio-bright, flat-spectrum population, which is most clearly associated with the GeV γ-ray sources. We seek to rectify this by defining CGRaBS, the Candidate Gamma-Ray Blazar Survey, a large sample of EGRET-like blazars selected across the extragalactic sky. By obtaining optical classifications and redshifts for a large fraction of these sources, we plan to enable prompt, intensive follow-up of the most interesting (e.g., high redshift, high luminosity, peculiar spectrum) sources that *are* detected in the LAT sky survey data. Furthermore, identification of a substantial fraction of the LAT sources with blazars will allow us to focus on the non-blazar remainder, potentially isolating new classes of cosmic γ-ray emitters.

2. Sample Selection

For any FoM-type counterpart selection, it is important to have uniform parent populations. Healey et al. (2007) have recently developed such a catalog, CRATES, which extended results of the CLASS survey (Myers et al. 2003) to obtain 8.4 GHz observations of all $|b| > 10^\circ$ objects brighter than 65 mJy at 4.8 GHz with spectral indices $\alpha > -0.5$ (where

$S \propto \nu^{\alpha}$). To estimate the radio spectral index of the core, we use the NVSS (Condon et al. 1998) and SUMSS (Bock et al. 1999) lower-frequency surveys. The result is a sample of over 11,000 flat-spectrum radio sources with interferometric measurements at ∼1 GHz and 8.4 GHz (with FWHM beam sizes ∼40″ and ∼0.25″ respectively), giving precise positions, spectral indices, and morphologies for the compact components. The CRATES catalog is as uniform as possible for the high-latitude ($|b| > 10°$) sky, limited by gaps in which the initial 4.8 GHz data are unavailable. We believe that this catalog is an excellent starting point for comparison with other all-sky samples (e.g., microwave and γ-ray).

Here we wish to find EGRET-like blazars, so we adopt the FoM of SRM03, which was derived from comparing the well-established 3EG blazar sources with the northern (CLASS-generated) subset of the CRATES catalog. This FoM is given by the heuristic fitting formula $\mathrm{FoM_{3EG}} = 100 \times P_\alpha \times P_S \times P_\mathrm{X} \times P_\mathrm{TS}$, where the P terms are "excess probabilities" for the observed parameters for radio sources near 3EG sources. Here, $P_\alpha = 0.19 - 0.35\alpha_{\mathrm{low/8.4}}$ ($0 \le P_\alpha \le 0.4$), $P_S = -3.47 + 2.45 \log_{10} S_{8.4} - 0.34 \log_{10}^2 S_{8.4}$ ($0 \le P_S \le 1$) and $P_\mathrm{X} = 0.99 + 0.41 \log_{10} F$ ($0.5 \le P_\mathrm{X} \le 1$), with F the RASS (Voges et al. 1999) counts per second and the P terms bounded to the ranges in parentheses. Finally, $P_\mathrm{TS} = 1 - \mathrm{CL}$, where CL is the confidence limit of the 3EG source localization contour passing through the position of the radio source. In essence, the FoM is composed of the product of the "excess" probabilities of sources of a given flux density, spectral index, etc. over random chance. While the FoM probability is not directly normalized, "false positive" rates were computed at each FoM level by comparison with the statistics of scrambled versions of the sky catalogs. Of course, once we have an initial survey of LAT blazar sources, it will be appropriate to derive new coefficients, "re-training" the FoM against this sample.

To develop an all-sky survey of blazar candidates, we compute an FoM for each source in the CRATES catalog. We must do this without reference to 3EG sources. Thus for this paper we define $\mathrm{FoM} = P_\alpha \times P_S \times P_\mathrm{X}$. To connect with $\mathrm{FoM_{3EG}}$, note that a blazar with the present FoM = 0.2 would correspond to a $\mathrm{FoM_{3EG}} = 1$ at the 95% localization contour of a γ-ray source, a "likely" (>90% correct) identification. With this definition, 5059 of the CRATES sources have a nonzero FoM. To focus our follow-up on the best and most 3EG-like objects, we define CGRaBS as those 1625 sources with FoM > 0.04. This corresponds to an SRM03 value of $\mathrm{FoM_{3EG}} = 2$ at the 50% localization contour, a very likely association, and a $\mathrm{FoM_{3EG}} = 0.2$ for a source at the 95% confidence contour, a reasonable (>80%) likelihood of an association. Figure 1 shows an Aitoff equal-area projection of the CGRaBS sample along with its parent survey, CRATES. Figure 2 shows a projection of the CGRaBS sample indicating the FoM of each source.

The radio spectral index is a major component of our FoM; thus, since the interfero-

metric observations at 8.4 GHz and low frequency were non-simultaneous, variability can, in principle, affect our FoM measurements. Luckily, the variability in the radio is modest compared to the high energy bands: Healey et al. found that the mean 8.4 GHz variability is $\leq$14% and the low-frequency variability on the relevant several-year timescale is even smaller. Thus, we do not expect that radio variability will dramatically affect our FoM estimates. Further, the (more likely variable) RASS detections turn out not to be a major selection bias in this survey. If the X-ray contribution to the FoM is ignored and a purely radio-based FoM is computed, then 98.5% of our sources still satisfy the CGRaBS FoM cutoff. Thus, while the X-ray flux from a small number of sources boosts them into the sample, the main effect of the X-ray contribution is to shuffle the ranking within the set of sources that are already qualified. Since the radio FoM weighting increases for bright and inverted (rising) spectra, its net effect is to impose an effective *extrapolated* flux density limit at a higher radio frequency. For example, the FoM = 0.04 cutoff corresponds to an extrapolated flux density at 100 GHz of $S_{100} > 230$ mJy (although we do not expect all sources to have a constant α to such high frequency). Less than 1% of the full CGRaBS targets have an extrapolated flux below this threshold, and these are all low-FoM sources with very high X-ray flux (i.e., largely high-peaked sources; see the next section).

Three CGRaBS sources warrant special comment. The CRATES entry for J0352−2514 is a combination of 8.4 GHz observations at two epochs, one with an unflagged mapping error and a grossly erroneous position. The CGRaBS entry for J0352−2514 uses only the good epoch to determine the correct position, the 8.4 GHz flux density, and the spectral index. Sources J0805−0111 and J1639+1632 have nominal CGRaBS spectral indices (and thus FoMs) that are almost certainly overestimates. Their NVSS counterparts have marginally resolved jet structure, and the NVSS decompositions offset the core toward the jet. A faint, spurious counter-jet component was introduced and, being slightly closer to the 8.4 GHz position, was selected as the 1.4 GHz counterpart, leading to a highly inverted spectral index and a high FoM. We include these sources in the survey since they satisfy the CGRaBS prescription; a more careful treatment of the NVSS counterparts would give a smaller spectral index and FoM. This effect is quite rare, occurring in CGRaBS for only these 2 sources (out of 1625, or 0.12%) and in CRATES for no more than 20 sources (out of 11,131, or 0.18%).

3. Optical follow-up

We have specifically *not* required a previous optical (or X-ray) detection of our blazar candidates. This radio-driven selection allows us to sample completely the flat-spectrum sources and avoid biasing the detected population. For example, X-ray–bright sources are

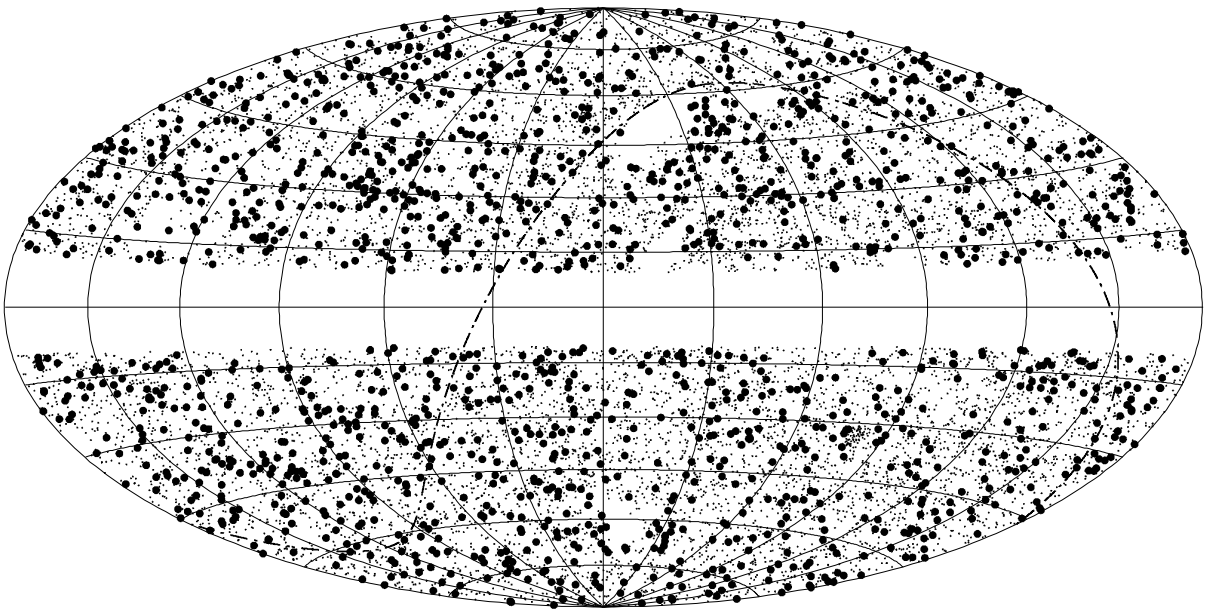

Fig. 1.— Aitoff equal-area projection of the CRATES parent sample (small dots) and the CGRaBS sample (large dots) in Galactic coordinates (l, b). The central meridian is $l = 0°$. A few small holes are visible just below $\delta = 0°$ (dot-dashed line), stemming from incomplete PMN sky coverage.

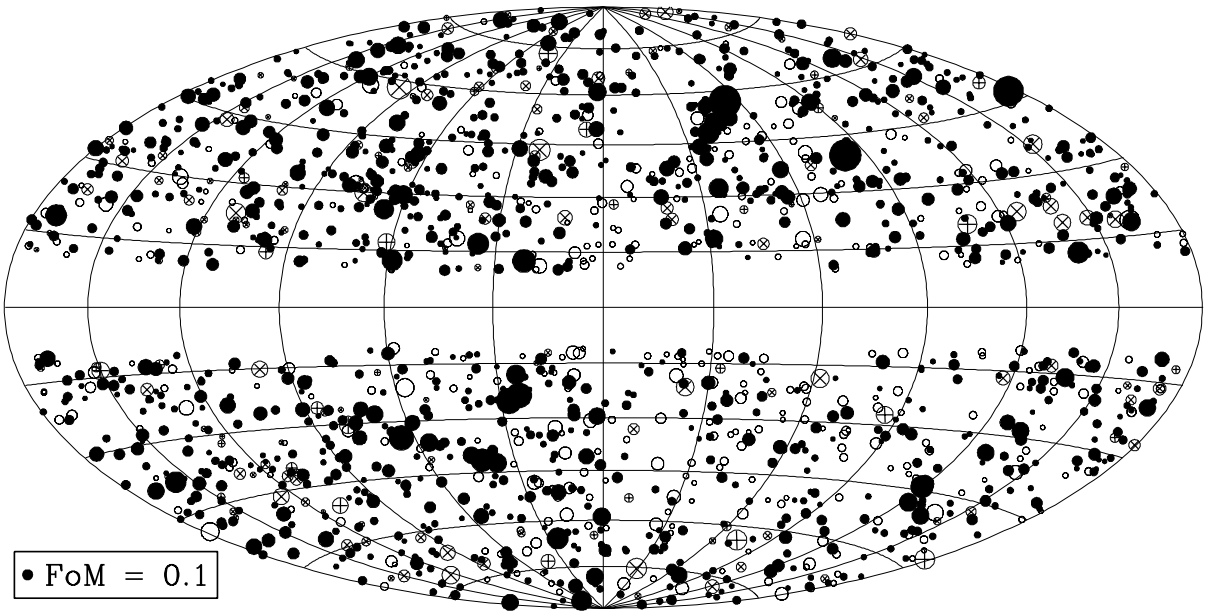

Fig. 2.— Aitoff equal-area projection of the CGRaBS sample in Galactic coordinates (l, b). The central meridian is $l = 0°$. The radius of each dot is proportional to the FoM of the source; the dot for a source with FoM = 0.1 is shown for comparison. The dot styles indicate optical classifications (see §§3.2.1-2): • = FSRQ, ⊗ = BLL, ⊕ = AGN, ∘ = unknown.

preferentially low-power "blue" blazars such as BL Lacs (so-called high-peaked blazars, or HBLs; Padovani & Giommi 1995). Similarly, requiring optically bright counterparts can bias the sample toward low redshift. However, since the principal goal of the CGRaBS project is to secure optical identifications, we do need good magnitude estimates. To maximize uniformity, we are working toward complete identification for $R < 23$. In practice, we have also observed a number of radio-bright and X-ray/γ-ray–bright but optically faint sources beyond this limit to explore the extrema of the population.

3.1. Counterparts and photometry

One defining blazar characteristic is rapid optical variability. Thus, we must set a fiducial "epoch" for the optical magnitudes. In practice, we use the USNO-B1 catalog (Monet et al. 2003) since this is the largest source of suitable R magnitudes; we take the fiducial magnitude to be that of the more sensitive second epoch survey (R2). Since we have precise radio positions for the cores of all sources, we identify a USNO-B1 source as the counterpart of a CGRaBS source if the optical position is within $1.5''$ of the radio position. This gives a large fraction of the required magnitudes, with completeness dropping between $R \sim 20$ and $R \sim 21$. For the north Galactic cap, we can supplement these with SDSS identifications (through Data Release 5, Adelman-McCarthy et al. 2007) to $r' \lesssim 22$. In confused cases, these archival data were examined visually to determine the best counterpart match. In a number of cases, we were also able to see clear counterparts that were too faint for inclusion in the USNO-B1 catalog but whose magnitudes could be reasonably estimated by measurement of the digitized plate data. In view of the variable blazar magnitudes and non-stellar colors, this low-precision photometry is adequate to guide the follow-up spectroscopy.

To complete the process of optical identification (and to improve a few poor USNO-B1 magnitudes), we have conducted our own imaging campaign, primarily at the 5 m Hale Telescope at Palomar, the 3.6 m New Technology Telescope (NTT) at La Silla, and the 2.7 m Harlan J. Smith Telescope at McDonald. Typical exposures were 180 s through Gunn r' under varying conditions, and magnitudes were calibrated against multiple field stars. For some particularly interesting sources (e.g., high radio-to-optical flux ratio candidates for high redshift), these were supplemented with *izJHK* imaging. We do not report here on these optical/IR SEDs. All r' magnitudes have been converted to R using the average color term ($R - r' = -0.253$) of CGRaBS sources detected by both the SDSS and USNO-B1. A magnitude (or limit) for each source is listed in Table 2. For some of the lowest redshift sources, the magnitude is dominated by the flux from the (extended) host galaxy. We also list the nominal Galactic extinction for the source direction A_R, derived from the Schlegel,

Finkbeiner & Davis (1998) maps. Even though the sources are at high latitude, there are a few targets behind dust clouds, indicating a large nominal extinction. However, we do not expect extinction to bias our measured population as the large A_R are not preferentially associated with the faint targets. Furthermore, only 4% of the blazars have $A_R > 1$ and 0.5% have $A_R > 2$; only 4 sources are excluded from the targeted $R = 23$ sample by the known extinction. As of 2007.5, there are 88 objects (5.4%) that do not have measured R magnitudes; of these, 45 have limits fainter than $R = 23$ and thus do not nominally require spectroscopy for the complete survey. The sources with brighter limits will be the subject of further imaging. Note that with 68 CGRaBS sources known to be fainter than $R = 23$, we expect that the survey will be >95% complete at this magnitude limit.

Figure 3 shows the distribution of R magnitudes and limits. Since the A_R are in general small, the extinction-corrected histogram is very similar. At first sight, the rapid drop between $20 < R < 21$ would seem to be due to the USNO-B1 survey completeness limit. However, we have sufficient deeper CCD imaging to determine that the drop in numbers is largely intrinsic, although we need to complete the imaging before we can characterize the details of the faint source distribution. The right panel shows that we need to complete identifications to faint magnitudes ($R > 19$) to get a representative sample of the higher redshift sources.

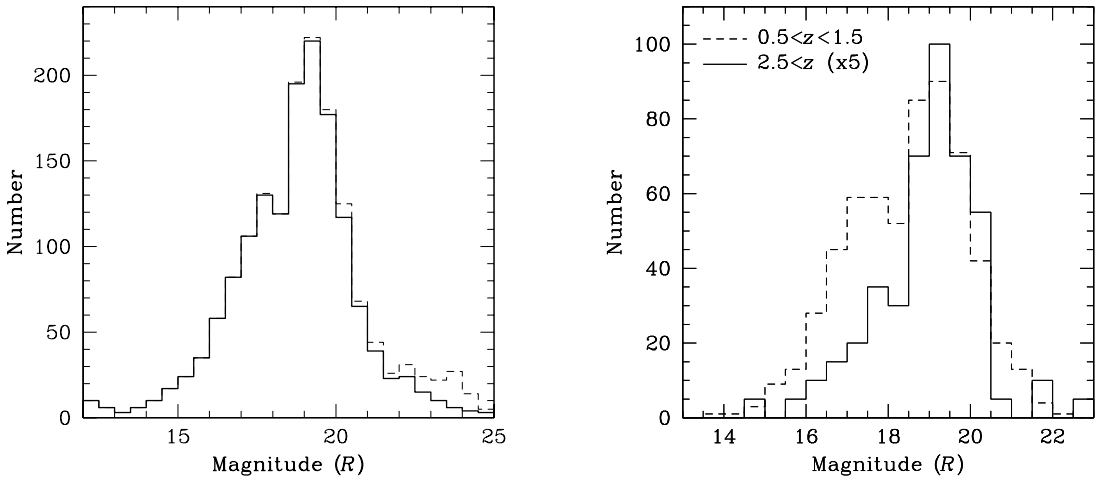

Fig. 3.— *Left:* Magnitude distribution of CGRaBS sources. Lower limits on R are shown by the dashed histogram. *Right:* Magnitude distributions for low-redshift and high-redshift sources.

3.2. Spectroscopy

Our spectroscopic goals are a basic classification of the AGN type, redshift measurement, and measurement of emission line equivalent strengths and kinematic widths (for luminosity and mass evolution studies). Thus, the bulk of our new observations have been low-resolution $\mathcal{R} \sim 500-1500$ long-slit spectroscopy. Most of the sources are flat-spectrum radio quasars whose broad lines allow easy identification with relatively low signal-to-noise. However, a significant fraction of the sources (∼15%) are weak-lined BL Lac sources. For these, we require high S/N and/or high resolution to determine the redshift from host absorption lines. Such measurements require long exposures with large telescopes. At present, we have identified sources as BL Lacs to $R \sim 20$, but our ability to measure the redshift drops significantly above $R \sim 18.5$; these BL Lacs are the subject of further spectroscopy at higher dispersion. In this paper, we present a progress report on the optical identifications. Additional papers will discuss the properties of the complete sample, the source SEDs, and the constraints on blazar evolution.

3.2.1. Observations

A fair fraction of the CGRaBS sources are bright, well-known AGN; thus, we have vetted our catalog against the twelfth edition of the Véron quasar catalog (Véron-Cetty & Véron 2006) and the SDSS DR5 quasar catalog (Schneider et al. 2007). We have also queried NED (`http://nedwww.ipac.caltech.edu/`) for all CGRaBS sources to find any other redshifts and identifications in the literature. Archival data identify ∼45% of the CGRaBS objects (∼60% of the redshifts in hand); the remainder are the targets of our own spectroscopic campaigns. The great workhorse of our spectroscopic effort has been the 9.2 m Hobby*Eberly Telescope (HET) at McDonald, which has observed hundreds of CGRaBS sources in the accessible declination band $-11^\circ < \delta < +73^\circ$. The telescope is fully queue-scheduled (Shetrone et al. 2007), allowing us to receive data remotely year-round and to spread the cost of inclement weather and unfavorable conditions. We use the Marcario Low Resolution Spectrograph (LRS; Hill et al. 1998) with grism G1 (300 lines mm^{-1}), $2''$ slit, and a Schott GG385 long-pass filter for a resolution of $\mathcal{R} \approx 500$. Typical exposures are 2×600 s, providing redshifts of emission-line objects to $R \sim 22$; brighter objects are also observed under poor conditions with 2×300 s.

In addition to our ongoing HET observations, we have mounted dedicated campaigns at a number of other facilities. We conducted three runs totaling 13 nights (over half lost to weather) on the 2.7 m Harlan J. Smith Telescope at McDonald, using the Imaging Grism Instrument (IGI) and the 6000 Å VPH grism. We observed 28 objects with the 1.5 m

telescope at Cerro Tololo in the "13/I" setup (grism 13, 150 lines mm^{-1}) in service observing mode as part of the Small and Medium Aperture Research Telescope System (SMARTS) program. We conducted two runs totaling 8 nights on the 3.6 m NTT at La Silla with the ESO Multi-Mode Instrument (EMMI) in the low-resolution spectroscopy (RILD) mode and grism 2 (300 lines mm^{-1}). To date, we have had three runs totaling 12 nights on the 5 m Hale Telescope at Palomar with the double spectrograph (DBSP), using a 300 lines mm^{-1} grating on the blue side and a 316 lines mm^{-1} grating on the red side. We observed 12 objects with the 8.2 m Kueyen telescope (the second unit telescope at the Very Large Telescope, VLT) in service observing mode with Focal Reducer/Low-Dispersion Spectrograph 1 (FORS1) and grism GRIS_300V (300 lines mm^{-1}). Finally, we have had three runs totaling 4 nights on the 10 m Keck I Telescope at Mauna Kea (however, the night of 2006 October 28 was the first observing night after the 2006 earthquake, and pointing was severely restricted; observations remained substantially constrained even on the night of 2006 November 24). For these observations, we used the Low Resolution Imaging Spectrometer (LRIS), employing a 600 lines mm^{-1} grism on the blue side and a 300 lines mm^{-1} grating on the red side. A summary of the observations is shown in Table 1.

The 1.5 m telescope observations were taken with a fixed N-S slit within a few hours of culmination. For all other systems, observations were taken with a long slit at the parallactic angle. Basic reduction steps were applied to the spectra using standard IRAF routines. Although every effort was made to minimize differential slit losses, in view of the variable slit widths and seeing, we have not attempted to derive absolute spectrophotometry. After standard star calibration, we estimate that the relative spectrophotometric accuracy is $\sim$30%, based on comparisons of observations of individual targets at different epochs with different instruments. Spectra were corrected for telluric absorption, and all observations for a given target were combined, weighted by S/N, to produce a final spectrum. Sample spectra are shown in Figure 4.

3.2.2. Results

Our spectral analysis starts with a basic source classification. The vast majority (84%) are flat-spectrum radio quasars (FSRQs) dominated by strong broad emission lines. The weak-lined BL Lac (BLL) class is somewhat heuristically defined; here we designate as BLLs sources that exhibit the following properties (Marchã et al. 1996): (1) emission line equivalent width < 5 Å, and (2) H/K 4000 Å break contrast $\equiv (f^+ - f^-)/f^+ < 0.4$, where f^+ (f^-) is the flux density redward (blueward) of the break. It is often possible to establish that a source is a BLL even when the redshift is impossible to determine. For sources with $R > 15$, we compute

Table 1. Summary of CGRaBS observations.

Telescope	Dates	Wavelength range (Å)	Spectral resolution (Å)	Typical seeing (arcsec)	Typical exposure (s)
9.2 m Hobby*Eberly	Ongoing, 2002–present	4100–9700	17	1.5	600, 1200
2.7 m Harlan J. Smith	2005 May 27–31	4250–8250	12	1.5	600, 1200
	2005 Oct 27–31	4250–8250	12	2.0	600, 1200, 1800
	2007 Mar 26–28	4250–8250	12	3.0	600, 1200, 1800
1.5 m CTIO	2005B	3500–9000	17	1.5	1200, 1800
3.6 m NTT	2006 Aug 29–Sep 1	3900–9100	10	1.3	600, 1800
	2007 Jan 22–25	3900–9100	10	1.0	600, 1200
5 m Hale	2005 Nov 5–9	3300–9500	5[a] , 16[b]	2.5	600, 1200
	2006 Aug 17–18	3300–9500	5[a] , 16[b]	1.7	600, 1200
	2007 Jan 15–16	3300–9500	5[a] , 16[b]	2.0	600, 1200
	2007 Apr 19–21	3300–9500	5[a] , 16[b]	2.5	600, 1200
8.2 m VLT-Kueyen	Period 78	3500–8000	17	1.2	600, 900, 1200, 1800
10 m Keck I	2006 Jul 22–23	3300–9300	3[a] , 11[b]	1.5	600, 1200
	2006 Oct 28	3300-9300	3[a] , 11[b]	1.5	600, 1200
	2006 Nov 24	3600-9600	3[a] , 11[b]	2.5	600, 1200

[a]Blue side.

[b]Red side.

M_R for the ΛCDM concordance cosmology (smaller R values are usually host-dominated, in any case) and classify broad emission line sources with $M_R > -23$ as AGN. Thus, we list here three blazar designations: continuum-dominated BLLs, low-luminosity broad-line AGN, and luminous broad-line FSRQs. A small number of non-blazar sources is also present. Sources with narrow lines ($v_{\rm FWHM} < 1000$ km s^{-1}) are denoted as narrow-line radio galaxies (NLRGs). Sources with small line equivalent widths but large H/K break contrasts are denoted as galaxies. These low-redshift sources may represent the low-luminosity extension of the blazar phenomenon. One extremely compact planetary nebula (PN) made our survey cuts. Finally, in four cases, the radio position was within 1.5″ of a field star that dominated the initial spectrum. With improved imaging, the fainter CGRaBS blazar counterparts can be identified.

Redshifts were measured by cross-correlation analysis. For a modest number of FSRQs, only a single strong, broad emission line is identified. In most cases, we conservatively identify this as Mg II λ2800, supported by the absence of strong lines expected for other identifications and, often, by Fe II structure in the surrounding continuum. Nevertheless, these redshifts are flagged by a colon (:), indicating possible systematic uncertainty. Absorption line redshifts were obtained for some BLLs. In a few cases, the BLL sources had multiple observations, and we were able to obtain emission line redshifts when the source was in a *low* continuum state and the emission line equivalent widths were relatively large. A few additional BLLs have redshift constraints, with upper limits from the lack of Ly-α absorption in the UV and lower limits from clearly identified (typically Mg II) intergalactic absorption systems. We have also measured continuum flux densities and equivalent and kinematic widths for the strong optical/UV resonance lines. These will be used to study the black hole masses and evolution.

Table 2 presents the first page of the CGRaBS catalog; the full table appears in the online edition. Here we include the precise position, the 8.4 GHz core flux density, the FoM, the R magnitude, the extinction A_R, and the optical classification and redshift, if any.

4. Discussion

To date, we have 1226 redshifts and 64 BLLs with unknown redshift. Thus classification is 79% complete with respect to the entire survey and 85% for objects with known $R < 23$. So far, 10.3% of all objects classified are BLLs, 3.4% are AGN, and 1% are NLRGs. Figure 5 shows the completeness as a function of magnitude. Source classification and redshifts are >85% complete to $R = 20$. While the completeness drops off rapidly beyond this, so do the source counts, and so reaching >95% completeness at the survey limit is feasible. Note,

Table 2. The CGRaBS catalog.

Name	R.A.[a]	Decl.[a]	$S_{8.4\,\mathrm{GHz}}$ (mJy)	FoM	X-ray flag[b]	R (mag)	A_R (mag)	Type[c]	z
J0001−1551	00 01 05.33	−15 51 07.1	335.90	0.050	–	18.09	0.08	FSRQ	2.044
J0001+1914	00 01 08.62	+19 14 33.8	504.20	0.105	–	20.50	0.11	FSRQ	3.100
J0003+2129	00 03 19.35	+21 29 44.4	269.70	0.098	–	19.75	0.12	AGN	0.450
J0004−1148	00 04 04.92	−11 48 58.4	774.90	0.112	–	19.09	0.08	BLL	
J0004+4615	00 04 16.13	+46 15 18.0	214.80	0.060	–	20.44	0.24	FSRQ	1.810
J0004+2019	00 04 35.76	+20 19 42.2	162.50	0.058	–	20.25	0.10	BLL	0.677
J0004−4736	00 04 35.68	−47 36 18.6	780.40	0.067	–	15.88	0.05	FSRQ	0.880
J0005−1648	00 05 17.93	−16 48 04.7	281.70	0.050	–	18.37	0.07		
J0005+0524	00 05 20.21	+05 24 10.7	228.90	0.066	–	16.26	0.08	FSRQ	1.900
J0005+3820	00 05 57.18	+38 20 15.2	1077.60	0.137	–	17.16	0.24	FSRQ	0.229
J0006−0623	00 06 13.89	−06 23 35.3	3296.90	0.135	–	17.14	0.10	BLL	0.347
J0006+2422	00 06 48.79	+24 22 36.5	230.90	0.049	–	18.71	0.24	FSRQ	1.684
J0008−2339	00 08 00.37	−23 39 18.1	377.20	0.057	–	16.16	0.05	FSRQ	1.410
J0008−4619	00 08 37.54	−46 19 40.8	176.00	0.041	–	16.51	0.04	FSRQ	1.850
J0010+2047	00 10 28.74	+20 47 49.7	272.10	0.071	–	18.41	0.23	FSRQ	0.600
J0010+1058	00 10 31.01	+10 58 29.5	245.00	0.141	–	12.22	0.26	AGN	0.089
J0010+1724	00 10 33.99	+17 24 18.8	867.50	0.069	–	16.90	0.10	FSRQ	1.601
J0010−3027	00 10 35.75	−30 27 47.4	316.70	0.050	–	19.07	0.04	FSRQ	1.189
J0010−2157	00 10 53.65	−21 57 04.2	358.90	0.049	–	19.68	0.06		
J0011−2612	00 11 01.25	−26 12 33.4	520.40	0.125	–	19.64	0.05	FSRQ	1.093
J0011+0057	00 11 30.40	+00 57 51.8	278.70	0.072	–	20.06	0.07	FSRQ	1.492
J0012+3353	00 12 47.38	+33 53 38.5	213.40	0.075	–	20.40	0.14	FSRQ	1.682
J0012−3954	00 12 59.91	−39 54 25.8	1554.20	0.181	–	18.05	0.03	BLL	
J0013−1513	00 13 20.71	−15 13 47.9	202.40	0.055	–	19.15	0.06	FSRQ	1.838
J0013−0423	00 13 54.13	−04 23 52.3	345.50	0.059	–	19.89	0.08	FSRQ	1.075
J0013+1910	00 13 56.38	+19 10 41.9	393.70	0.110	–	18.17	0.13	BLL	
J0015−1812	00 15 02.49	−18 12 50.9	378.30	0.054	–	19.65	0.09	FSRQ	0.743
J0016−0015	00 16 11.09	−00 15 12.5	732.50	0.040	–	19.72	0.08	FSRQ	1.574
J0017+8135	00 17 08.48	+81 35 08.1	1361.10	0.140	–	15.95	0.49	FSRQ	3.387
J0017−0512	00 17 35.82	−05 12 41.7	225.20	0.050	–	17.60	0.08	FSRQ	0.227
J0019+2021	00 19 37.85	+20 21 45.6	1232.90	0.098	–	19.70	0.16	BLL	
J0019−3031	00 19 42.67	−30 31 18.6	485.40	0.058	–	19.64	0.06	FSRQ	2.677
J0019+2602	00 19 39.78	+26 02 52.3	458.50	0.046	X	15.04	0.08	FSRQ	0.284
J0019+7327	00 19 45.79	+73 27 30.0	1330.70	0.094	–	18.26	0.86	FSRQ	1.781
J0022+4525	00 22 06.61	+45 25 33.8	307.50	0.043	–	20.72	0.19	FSRQ	1.897
J0022+0608	00 22 32.44	+06 08 04.2	301.20	0.052	–	19.07	0.06	BLL	
J0023+4456	00 23 35.44	+44 56 35.8	240.00	0.065	–	21.70	0.16	FSRQ	1.062
J0024+2439	00 24 27.33	+24 39 26.3	188.00	0.040	–	19.20	0.08	FSRQ	1.444
J0025−2227	00 25 24.25	−22 27 47.6	248.80	0.052	–	18.73	0.04		
J0026−3512	00 26 16.39	−35 12 48.7	314.70	0.108	–	19.68	0.03		
J0027+2241	00 27 15.37	+22 41 58.2	323.80	0.055	–	15.60	0.10	FSRQ	1.108

[a] J2000.0 position.

[b] "X" indicates that a source would not satisfy the FoM cutoff if its X-ray flux were ignored. See §2.

[c] See §§3.2.1-2 for discussion of the type classifications.

however, that only ∼52% of the BLLs have redshifts and that this fraction falls off quickly above $R = 18$. Clearly, pushing the largely complete BLL sample fainter than $R = 20$ will be a challenge.

We defer full discussion of the sample properties until we reach our expected 95% completeness to $R = 23$. However, it is already interesting to examine the redshift distribution of the sources detected to date (Figure 6). The non-BLL (largely FSRQ) distribution peaks at $z \approx 1.3$ and has an exponential fall-off ($\mathrm{d}N/\mathrm{d}z \propto 10^{-0.6z}$) to high redshift, extending to $z = 5.5$. From SED information on optically faint sources, we expect the high-redshift population to increase somewhat in the complete CGRaBS sample, but it is clear that there will be only a handful of radio-bright blazars at $z > 4$. If any of these are detected by the LAT, as expected, they will be particularly important targets for multiwavelength spectral and variability studies. In fact, with only ∼40 sources at $z > 3$, careful study of these few high-redshift objects will be important for several LAT programs, e.g., extragalactic background light (EBL) studies and studies of jet evolution and interaction with the CMBR.

We are also assembling an important new sample of radio-bright BLLs. To date, we have 133 sources definitively classified as BLLs, but this will likely grow since a substantial number of other sources have observed BLL-like spectra but need somewhat improved S/N observations to exclude emission lines with EW ≥ 5 Å throughout the observed spectrum. Among the brighter sources ∼15% are BLL; at this incidence, we expect ∼245 sources to have a final BLL classification. As noted, it will be very tough to obtain redshifts of the faintest BLLs. However, the 70 redshifts already in hand represent a substantial radio-bright sample. For example, it is twice the size of the 1 Jy sample (Stickel et al. 1991) and extends to nearly twice the redshift. At present, we have 11 BLLs at $z > 1$, a third of all known $z > 1$ BLLs, so that the full survey should be useful for probing evolution of this population.

Of course, the most important application of the CGRaBS catalog is the identification with other all-sky samples and the generation of multiwavelength SEDs. We are already examining the radio to X-ray spectra of these sources and eagerly look forward to the upcoming sky surveys with *AGILE*, the air-Čerenkov TeV observatories, and especially *GLAST*, which will measure the γ-ray power peak expected for many of these sources.

S. E. H. was supported by SLAC under DOE contract DE-AC03-76SF00515.

The Hobby*Eberly Telescope (HET) is a joint project of the University of Texas at Austin, the Pennsylvania State University, Stanford University, Ludwig-Maximilians-Universität München, and Georg-August-Universität Göttingen. The HET is named in honor of its principal benefactors, William P. Hobby and Robert E. Eberly.

The Marcario Low Resolution Spectrograph is named for Mike Marcario of High Lonesome Optics, who fabricated several optics for the instrument but died before its completion. The LRS is a joint project of the Hobby*Eberly Telescope partnership and the Instituto de Astronomía de la Universidad Nacional Autónoma de México.

This paper includes data taken at the McDonald Observatory of the University of Texas at Austin.

The data in this paper are based partly on observations obtained at the Hale Telescope, Palomar Observatory, as part of a collaborative agreement between the California Institute of Technology, its divisions Caltech Optical Observatories and the Jet Propulsion Laboratory (operated for NASA), and Cornell University.

Some of the data presented herein were obtained at the W. M. Keck Observatory, which is operated as a scientific partnership among the California Institute of Technology, the University of California and the National Aeronautics and Space Administration. The Observatory was made possible by the generous financial support of the W. M. Keck Foundation.

The authors wish to recognize and acknowledge the very significant cultural role and reverence that the summit of Mauna Kea has always had within the indigenous Hawaiian community. We are most fortunate to have the opportunity to conduct observations from this mountain.

Some of the data in this paper are based on observations made with ESO telescopes at the La Silla Observatory under program 077.B-0056(A) and ID 078.B-0275(B).

Funding for the SDSS and SDSS-II has been provided by the Alfred P. Sloan Foundation, the Participating Institutions, the National Science Foundation, the U. S. Department of Energy, the National Aeronautics and Space Administration, the Japanese Monbukagakusho, the Max Planck Society, and the Higher Education Funding Council for England. The SDSS Web site is `http://www.sdss.org/`.

The SDSS is managed by the Astrophysical Research Consortium for the Participating Institutions. The Participating Institutions are the American Museum of Natural History, Astrophysical Institute Potsdam, University of Basel, University of Cambridge, Case Western Reserve University, University of Chicago, Drexel University, Fermilab, the Institute for Advanced Study, the Japan Participation Group, Johns Hopkins University, the Joint Institute for Nuclear Astrophysics, the Kavli Institute for Particle Astrophysics and Cosmology, the Korean Scientist Group, the Chinese Academy of Sciences (LAMOST), Los Alamos National Laboratory, the Max Planck Institute for Astronomy (MPIA), the Max Planck

Institute for Astrophysics (MPA), New Mexico State University, Ohio State University, University of Pittsburgh, University of Portsmouth, Princeton University, the United States Naval Observatory, and the University of Washington.

This research has made use of the NASA/IPAC Extragalactic Database (NED), which is operated by the Jet Propulsion Laboratory, California Institute of Technology, under contract with the National Aeronautics and Space Administration.

REFERENCES

Adelman-McCarthy, J. et al. 2007, ApJS, in press.

Bock, D. C.-J., Large, M. I., & Sadler, E. M. 1999, AJ, 117, 1578.

Condon, J. J. et al. 1998, AJ, 115, 1693.

Hartman, R. C. et al. 1993, ApJ, 407, L41.

Hartman, R. C. et al. 1999, ApJS, 123, 79.

Healey, S. E. et al. 2007, ApJS, 171, 61.

Hill, G. J. et al. 1998, SPIE, 3355, 375.

Kniffen, D. A. et al. 1993, ApJ, 411, 133.

Marchã, M. J. M. et al. 1996, MNRAS, 281, 425.

Massaro, E. et al. 2007, `http://www.asdc.asi.it/bzcat/`

Mattox, J. R. et al. 2001, ApJS, 135, 155.

Monet, D. G. et al. 2003, AJ, 125, 984.

Myers, S. T. et al. 2003, MNRAS, 341, 1.

Padovani, P. & Giommi, P. 1995, ApJ, 444, 567.

Schneider, D. P. et al. 2007, AJ, 134, 102.

Schlegel, D. J., Finkbeiner, D. P. & Davis, M. 1998, ApJ, 500, 525.

Shetrone, M. et al. 2007, PASP, 119, 556.

Sowards-Emmerd, D. et al. 2003, ApJ, 590, 109.

Sowards-Emmerd, D. et al. 2005, ApJ, 626, 95.

Stickel, M. et al. 1991, ApJ, 374, 431.

Turriziani, S. et al. 2007, astro-ph/0705.1498.

Véron-Cetty, M.-P. & Véron, P. 2006, A&A, 455, 773.

Voges, W. et al. 1999, A&A, 349, 389.

This preprint was prepared with the AAS LaTeX macros v5.2.

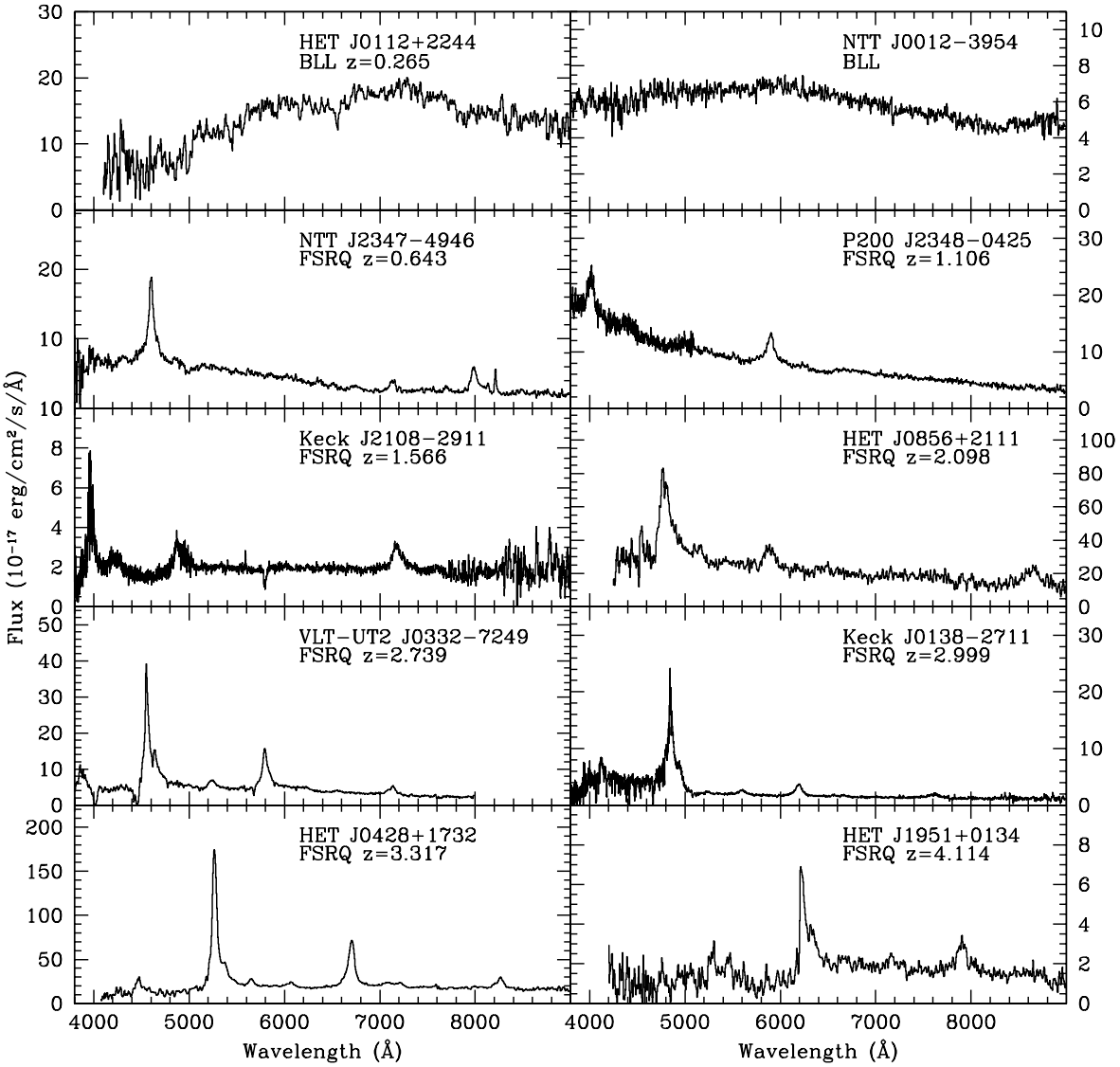

Fig. 4.— Sample CGRaBS spectra.

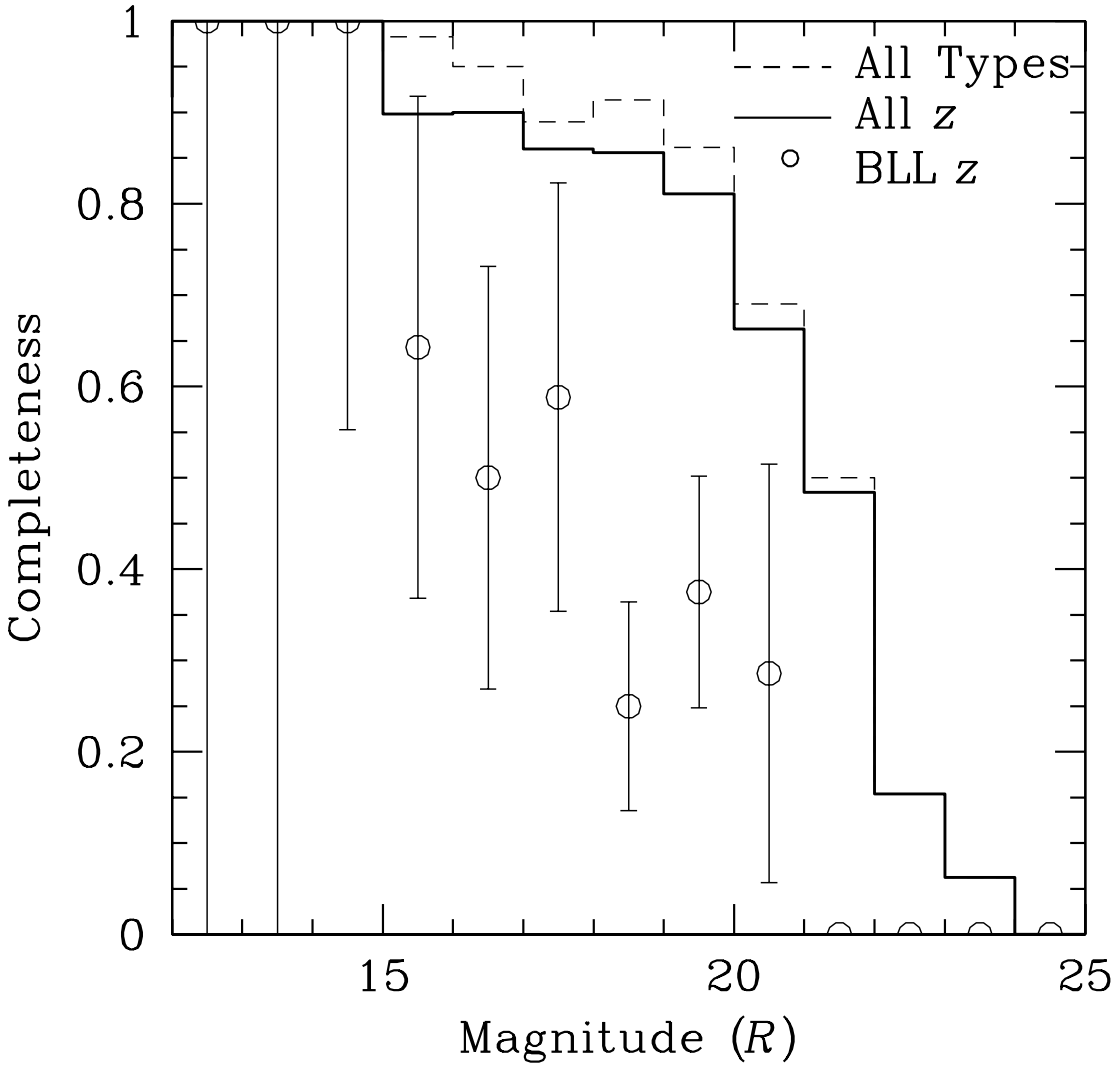

Fig. 5.— Completeness as a function of R for source identification and redshift measurement (histograms). The points show the fraction of identified BLL with measured redshift; small numbers lead to substantial error bars.

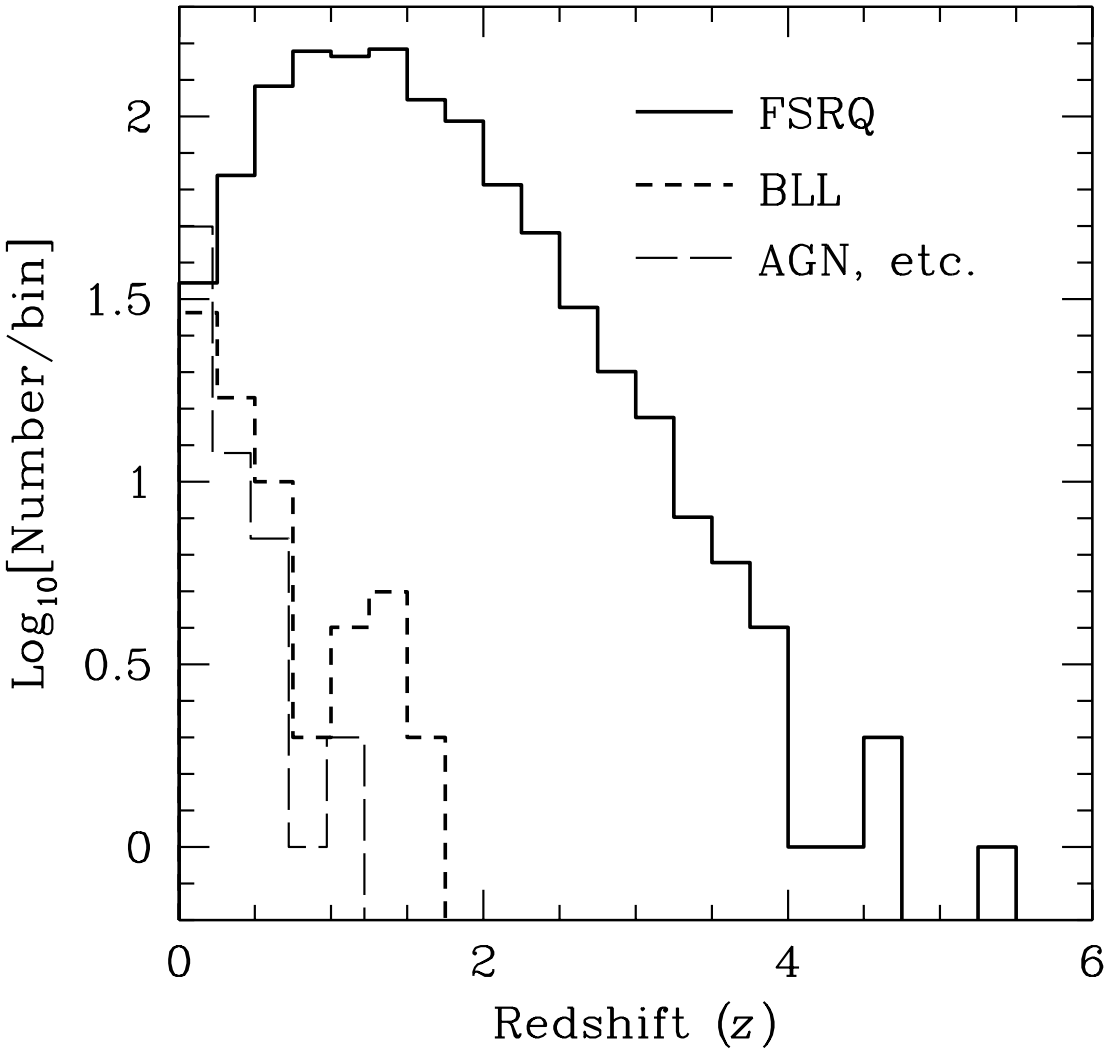

Fig. 6.— Redshift distributions for the (partly complete) CGRaBS survey. The solid-line histogram shows FSRQs. The short-dashed histogram gives the redshift distribution for solved BLLs. The long-dashed histogram shows a variety of other AGN (NLRGs, passive ellipticals, etc.), which contribute only at very low redshift.